Adhesion properties of chain-forming ferrofluids

Sérgio A. Lira and José A. Miranda*
Departamento de Física, LFTC, Universidade Federal de Pernambuco, Recife, Pernambuco 50670-901, Brazil
(Received 13 November 2008; revised manuscript received 28 January 2009; published 2 April 2009)

Denser and highly magnetized ferrofluids exhibit several non-Newtonian behaviors attributed to the formation of magnetic particle chains. We investigate the rheological and adhesive properties during tensile deformation of a confined chain-forming ferrofluid subjected to a radial magnetic field. Both the magnetoviscous contribution to the viscosity and the adhesive force are derived analytically. The response of the system to changes in the length of the chains is examined under zero and nonzero shear circumstances. Our results indicate that the existence of chains has a significant impact on the adhesive strength as well as on the viscosity of the ferrofluid, allowing it to display both shear-thinning and shear-thickening regimes. These findings open up the possibility of monitoring complex rheological responses of such fluids with the assistance of applied magnetic fields, allowing a more accurate assessment of their adhesive properties.

DOI: 10.1103/PhysRevE.79.046303 PACS number(s): 47.65.Cb, 75.50.Mm, 68.35.Np, 47.20.Gv

I. INTRODUCTION

The detailed understanding of a number of adhesion processes is made difficult by the inherent complexity of adhesive materials. Typical adhesives are based on weakly crossed-linked high-molecular weight polymers and present very intricate rheological properties, many of them often not fully known [1,2]. A convenient way of approaching the complicated effects in conventional soft adhesives has been recently tackled by some research groups which examined the fundamentals of adhesion in viscous fluids [3–10]. In these studies it has been demonstrated that, although fluids are not, rigorously speaking, "true" adhesives they present physical properties that are quite similar to the ones of regular soft adhesives. Initially, the simplest situation of Newtonian fluids has been considered, and then different levels of rheological complexity have been added to gain some appreciation for the fluid nature of more traditional adhesive processes.

One efficient and relatively simple method to access and characterize important adhesive properties both in conventional adhesives as well as in viscous fluids is provided by the so-called probe-tack test [11,12]. In the "plate-plate" version of this test a sample of material is first confined between two parallel plane plates, and then the upper plate is lifted at a known rate while the applied force is recorded. When the upper plate is lifted, the pressure gradient causes an inward viscous shearing flow in the plane of the adhesive or fluid film, producing a downward adhesive force normal to the upper plate. The result is a force-distance curve that quantifies the adhesive strength of the sample under tension as a function of the upper plate displacement. The debonding studies performed in Refs. [3–10] have made ample use of the probe-tack test to gain insight into the adhesive properties of viscous fluids.

Among the investigations that consider the fluid nature of adhesion, one is particularly compelling, in the sense that it addresses adhesion phenomena in magnetic fluids [10]. In contrast to Refs. [3–9] in which the fluid under study is nonmagnetic, in Ref. [10] the material is a viscous Newtonian ferrofluid subjected to an external magnetic field. Ferrofluids [13,14], which are stable colloidal suspensions of magnetic nanoparticles respond paramagnetically to applied magnetic fields. The interplay between fluid dynamic and magnetic contributions in ferrofluids leads to various interesting field-induced behaviors and pattern formation processes. It has been shown [10] that, contrary to conventional adhesive materials, the adhesive properties of a ferrofluid can be enhanced or reduced by varying the intensity or symmetry configuration of externally applied magnetic fields. Another possibility of magnetically tuning the system can be accomplished by manipulating the material properties of the ferrofluid. All this established a suggestive connection between adhesion and ferrohydrodynamic phenomena, allowing the control of important adhesive properties by magnetic means.

However, no systematic study of the adhesion phenomena in ferrofluids focusing on the role of their rheological properties or possible non-Newtonian behavior has been undertaken so far. In fact, the viscosity of the ferrofluid contemplated in Ref. [10] is assumed to be constant, and therefore independent of the magnetic field. Consequently, the influence of eventual rheological effects related to field- and shear-dependent changes in the viscosity of the magnetic fluid [13–17] has not been considered. On the other hand, the recent development of denser and more strongly magnetized ferrofluids has revealed a wide range of non-Newtonian behaviors in these liquids, such as shear-thinning, shear-thickening, normal stress differences, viscoelastic response, and a varying (Trouton) elongational viscosity. These various rheological manifestations have been scrutinized both experimentally [18,19] and theoretically [17,20–24] and are attributed to the formation of short chains when the magnetic particles are exposed to strong magnetic fields. This effect can be modeled by a polydisperse ferrofluid consisted of a small portion of larger particles forming short chains, causing the fluid to display non-Newtonian behavior, plus a large portion of smaller particles which determine the overall magnetic properties of the fluid.

In this work we analyze the adhesion properties of a chain-forming, non-Newtonian ferrofluid subjected to a spe-

*jme@df.ufpe.br

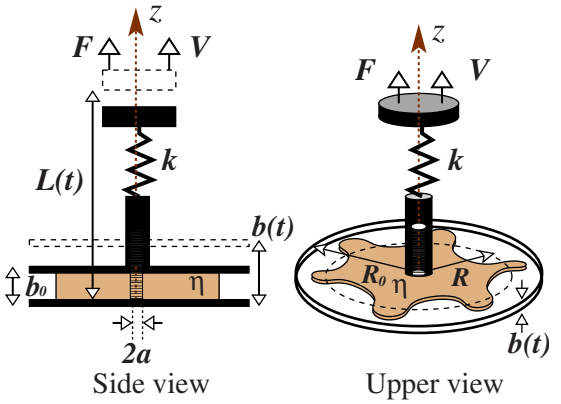

FIG. 1. (Color online) Diagrammatic representation of the probe-tack apparatus, where a non-Newtonian ferrofluid of viscosity η is confined between parallel plates and subjected to a radial magnetic field. The surrounding fluid is nonmagnetic and inviscid.

cifically designed magnetic-field configuration, which tends to empower the action of magnetic effects as the inward ferrofluid flow progresses during a probe-tack test. The investigation of this particular debonding event allows us to examine how magnetic field, viscous shear, and short chain formation affect the ferrofluid's viscosity and its adhesive strength. In a more general sense, in addition to helping for a better understanding of non-Newtonian phenomena in magnetic fluids, our study bridges the research areas of adhesion, rheology, and ferrohydrodynamics which are by themselves vastly interdisciplinary.

II. ADHESION FORCE: MAGNETOVISCOUS AND PARTICLE CHAIN-FORMATION EFFECTS

Figure 1 sketches the geometry of the probe-tack system. We consider a non-Newtonian, incompressible ferrofluid of viscosity η located between two narrowly spaced circular, flat plates. The outer fluid is nonmagnetic and of negligible viscosity. As in Refs. [3–5,10] we consider that the apparatus has a spring constant denoted by k. One end of the lifting apparatus moves at a specified constant velocity V, subjecting the upper plate to a pulling force F. The lower plate is held fixed at $z=0$, where the z axis points in the direction perpendicular to the plates. The initial plate-plate distance is represented by b_0 and the initial ferrofluid radius by R_0. At a given time t the plate spacing is $b=b(t)$, while the deformation due to the stretching of the apparatus is $L-b$, where $L=b_0+Vt$. Due to the compliance of the measurement apparatus, the actual plate spacing b is not necessarily equivalent to L. Of course, in the case of a completely rigid apparatus we have $b=L$ and $\dot{b}=V$, where $\dot{b}=db/dt$.

The ferrofluid sample is subjected to a cylindrically radial applied magnetic field given by [25,26]

$$\mathbf{H}_a = \frac{H_0 a}{r}\hat{\mathbf{r}}, \tag{1}$$

where a is the radius of magnetic-field source, r is the radial distance from the origin of the coordinate system (located at the center of the ferrofluid sample), H_0 is a constant, and $\hat{\mathbf{r}}$ is a unit vector in the radial direction. The experimental conditions required to obtain such a radial magnetic field are discussed in Ref. [25]. Notice that this field configuration ($H_a \sim 1/r$) is particularly convenient to examine the magnetic field induced changes in the viscosity of the ferrofluid: during the probe-tack test, as the plates separate and the magnetic fluid move radially inward, the magnetic field becomes increasingly stronger inducing more significant magnetoviscous effects.

Our main goal is to calculate the pulling force F as a function of displacement L, taking into account both hydrodynamic and magnetic contributions. First, we calculate F analytically for the completely rigid case, and subsequently we address the more realistic situation in which compliance is taken into consideration, by performing a numerical calculation. We follow Refs. [4,7] and derive F assuming that the ferrofluid interface remains circular during the entire lifting process, with time-dependent radius defined as $R=R(t)$. Conservation of ferrofluid volume leads to the relation $(R^2-a^2)b=(R_0^2-a^2)b_0$.

If we assume that the upper plate is not being lifted fast enough to incite any inertial effects, nor lifted high enough to alter the system being of large aspect ratio $[R(t) \gg b(t)]$ a modified Darcy's law applies [10,27],

$$\mathbf{v} = -\frac{b^2}{12\eta}\boldsymbol{\nabla}[p-\Psi], \tag{2}$$

where $\mathbf{v}(r,\theta)$ represents the quasi-two-dimensional flow between the separating plates, p is the hydrodynamic pressure, and Ψ denotes a magnetic pressure represented by a scalar potential. The probe-tack test setup defines a particular type of flow in which the velocity field is vorticity-free and can be written (in polar coordinates) as $\mathbf{v}=(-\dot{\varepsilon}r/2,0)$, where the shear rate parameter $\dot{\varepsilon}=\dot{b}/b$ quantifies the flow (or, elongation) rate.

Our first task is to compute the viscosity η appearing in Eq. (2) and find out how it is influenced by the applied magnetic field, and also by other relevant effects connected to magnetic particle chain-formation and viscous shear. We follow Refs. [23,24,28] and assume that the total viscosity is related to the normal stress difference at finite shear, subtracted from its corresponding value at vanishing shear,

$$\eta = \eta_0 + \eta_m = -\frac{[T_{rr} - T_{rr}|_{\dot{\varepsilon}=0}]}{\dot{\varepsilon}}, \tag{3}$$

where η_0 denotes the viscosity at zero magnetic field and η_m represents the magnetoviscous contribution. We call the reader's attention to the fact that, unlike previous theoretical studies [23,24], our applied magnetic field is nonuniform, possessing a radial gradient. Consequently, the basic rheological responses found in Refs. [23,24], which are quite sensitive to the symmetry properties of the imposed magnetic field, cannot be assumed *a priori* as valid for our system.

The total stress tensor including viscous and magnetic effects is defined as [13,14,23,24]

$$T_{ij} = -\tilde{p}\delta_{ij} + 2\eta_0 \mathrm{v}_{ij} + H_i B_j - \frac{1}{2}[(M_i h_j - M_j h_i) - \lambda_2 (M_i h_j + M_j h_i)], \tag{4}$$

where δ_{ik} denotes the Kronecker delta function and the parameter $\tilde{p}=p+\Psi+\mu_0 H^2/2$ with

$$\Psi = \mu_0 \int_0^H M dH, \tag{5}$$

where μ_0 denotes the magnetic permeability of free space. In addition, $\mathrm{v}_{ij}=(\nabla_i \mathrm{v}_j + \nabla_j \mathrm{v}_i)/2$, $\mathbf{H}$ is the magnetic field, $\mathbf{B}$ is the magnetic-field induction, $\mathbf{M}$ is the magnetization, and $\mathbf{h}=\mathbf{M}/\chi-\mathbf{H}$, with χ denoting the ferrofluid's susceptibility. The transport coefficient λ_2 [17], which is a very important quantity for our investigation, accounts for the influence of the elongational flow, in the sense that the flow induced by the lifting of the upper plate yields a torque acting on existing chains, interfering on the rheological properties of the ferrofluid. The value of λ_2, which lies between 0 and 1, has been related to the length of the magnetic particle chains [20,29], where $\lambda_2 \to 0$ corresponds to chainless (single particle) ferrofluids, and $\lambda_2 \to 1$ would be associated to the formation of chains (in a polydisperse ferrofluid) with a mean length of approximately five particles.

Another key ingredient for our calculation is the relaxation equation for the magnetization [17]

$$\frac{dM_i}{dt} + (\mathbf{M}\times\mathbf{\Omega})_i - \lambda_2 M_j \mathrm{v}_{ij} = -(M_i - M_i^{\mathrm{eq}})/\tau, \tag{6}$$

where $\mathbf{\Omega}=(\nabla\times\mathbf{v})/2$ is the vorticity of the flow, $M_i^{\mathrm{eq}}=\chi H_i$ is a linear constitutive relation for the equilibrium magnetization, and τ is the relaxation time for the magnetization. Note that if $\lambda_2=0$ Eq. (6) reduces to the classical relaxation equation derived by Shliomis [15,16]. Since in our present case $\mathbf{\Omega}=0$, and considering the stationary situation for which $d\mathbf{M}/dt=0$, we can use Eq. (6) plus the fact that the tangential component of $\mathbf{H}$ and the normal component of $\mathbf{B}$ are both continuous at the fluid-fluid interface, to get

$$\mathbf{M} = \chi\Gamma\mathbf{H}_a, \tag{7}$$

with $\Gamma=\Gamma(\chi,\lambda_2,\xi)=1/[1+\chi+(\lambda_2\xi/2)]$, where $\xi=\tau\dot{\epsilon}$ defines a dimensionless shear rate. Moreover, with the help of Eqs. (5) and (7) we can write the proper scalar potential for the radial field configuration as

$$\Psi(r) = \frac{\mu_0}{2}\chi\Gamma(1-\chi\Gamma)H_a^2. \tag{8}$$

At this point we have all elements we need to evaluate the magnetoviscous contribution to the total viscosity. By substituting Eq. (7) into the formula for the total stress tensor Eq. (4), and then using the resulting expression for T_{rr} into Eq. (3) we obtain

$$\eta_m = -\frac{1}{2}\frac{\chi\lambda_2\tau H_a^2}{[1+\chi+(\lambda_2\xi/2)]^2}\left[1-\lambda_2+\frac{\lambda_2\xi}{2(1+\chi)}\right]. \tag{9}$$

This expression reveals a suggestive coupling between the magnetic particle chain formation parameter λ_2 and the dimensionless shear rate ξ. Since $0<\lambda_2<1$ we notice that $\eta_m \le 0$, and tends to zero if the magnetic particle chains are not formed ($\lambda_2 \to 0$). Therefore, the non-Newtonian character of the ferrofluid is intimately related to the very existence of chains. Furthermore, observe that in the limit of very small shear ($\xi \to 0$) η_m assumes a simpler form, depending quadratically on λ_2 [$\eta_m \sim \lambda_2(1-\lambda_2)$].

The determination of the pressure field is a fundamental step toward the calculation of the adhesion force. Fortuitously, it can be readily computed by inserting Eq. (9) into Darcy's law Eq. (2), and integrating with respect to r yielding

$$p(r) = \frac{3\eta_0 \dot{b}}{b^3}\left\{(r^2-R^2) - \frac{\lambda_2\tau\chi\Gamma^2 a^2 H_0^2}{\eta_0}\left[1-\lambda_2+\frac{\lambda_2\xi}{2(1+\chi)}\right]\ln\left(\frac{r}{R}\right)\right\} + [\Psi(r)-\Psi(R)] + p(R), \tag{10}$$

where $p(R)$ is the value of the pressure at the ferrofluid droplet boundary. To determine $p(R)$ we use the fact that $\Psi=0$ in the nonmagnetic fluid, and the generalized pressure jump condition which expresses the equilibrium condition on the normal component of the local stress tensor across the fluid-fluid interface [13,14]

$$\mathbf{n}\cdot\Delta\boldsymbol{T}\cdot\mathbf{n} = \sigma\kappa, \tag{11}$$

where T_{ij} is given in Eq. (4) and $\mathbf{n}$ denotes the unit normal vector at the interface. The term at the right-hand side of Eq. (11) represents the contribution related to surface tension and interfacial curvature κ. By utilizing Eqs. (11), (7), and (4) we get

$$p(R) = p_0 - \frac{\mu_0}{2}\chi\Gamma[1+\Gamma(1-\chi\Gamma)^2\lambda_2^2\xi]H_a^2|_{r=R}, \tag{12}$$

where p_0 denotes the constant pressure outside the ferrofluid droplet. In deriving Eq. (12), as is common in this type of adhesion phenomena [3–7], we have neglected the surface tension term.

The force exerted by the lifting machine on the upper plate is calculated by integrating the total stress difference above and below the upper plate, yielding

$$F = \int [\hat{\boldsymbol{z}}\cdot\boldsymbol{T}^{\mathrm{ff}} - \hat{\boldsymbol{z}}\cdot\boldsymbol{T}^{\mathrm{out}}]\cdot\hat{\boldsymbol{z}} dA = \int_a^R [T_{zz}^{\mathrm{ff}}(r) - T_{zz}^{\mathrm{out}}(r)] 2\pi r dr, \tag{13}$$

where $\hat{\boldsymbol{z}}$ is a unit vector in the z direction, $\boldsymbol{T}^{\mathrm{ff}}$ denotes the total stress tensor at the ferrofluid surface in contact with the upper plane, whereas $\boldsymbol{T}^{\mathrm{out}}$ represents the corresponding stress tensor due to the outer nonmagnetic fluid. The integration is carried out over the cross-sectional area of the ferrofluid drop A. Under such circumstances, by using Eq. (4) the evaluation of Eq. (13) leads to a *dimensionless* force

$$F = \frac{\dot{b}}{b^5}\left\{\left(\frac{\gamma-1}{\gamma}\right)^2 - \frac{N_N}{\gamma^2}\Delta\left[\frac{b}{b_0}(\gamma-1) - \frac{b^2}{b_0^2}\ln\left(1+(\gamma-1)\frac{b_0}{b}\right)\right]\right\} + N_B\chi\Gamma\left[\Lambda\frac{(\gamma-1)}{\frac{b}{b_0}+(\gamma-1)} + \chi\Gamma\ln\left(1+(\gamma-1)\frac{b_0}{b}\right)\right], \quad (14)$$

where $\gamma=(R_0/a)^2$, $N_N=\tau H_0^2/\eta_0$ is a non-Newtonian Bond number related to the non-Newtonian character of the viscosity, and $N_B=(\pi\mu_0 H_0^2 a^2)/(2k\delta)$ is a magnetic Bond number for the radial magnetic-field configuration. The parameters Γ, $\Delta=-2\eta_m/(\tau H_a^2)>0$, and $\Lambda=2-\chi\Gamma+\Gamma(1-\chi\Gamma)^2\lambda_2^2\xi>0$ couple χ, ξ, and λ_2. Similar to what is done in Refs. [3,4], in Eq. (14) lengths have been rescaled by $\delta=(3\pi\eta_0 R_0^4 b_0^2 V/2k)^{1/6}$ and velocities by V. In addition, the adhesion force is rescaled by $k\delta$. It is worth mentioning that since we are dealing with the noncompliant situation, we have $b=L$ and hence $\dot{b}=1$. Equation (14) shows $\dot{b}$ explicitly in anticipation of our analysis of the compliant apparatus situation.

Equation (14) for the adhesion force and Eq. (9) for the magnetoviscous contribution to the total viscosity are central results of this work. The basic physical effects present in the adhesion force equation can be understood simply by looking at the sign of the magnetic terms N_N and N_B. Positive magnetic terms which are multiplied by N_B in Eq. (14) lead to increased adhesion while negative terms proportional to N_N lead to decreased adhesion. The first term on the right-hand side of Eq. (14) is related to the usual purely viscous contribution in the absence of any magnetic effects. The nontrivial interplay of these contributions will dictate the final outcome for the rheological and adhesive properties of the non-Newtonian ferrofluid.

III. DISCUSSION

In order to strengthen the practical and academic relevance of our theoretical study, we ensure that the values of all relevant dimensionless quantities we utilize are consistent with realistic physical parameters related to existing probe-tack test instruments [3–7], radial magnetic-field arrangement [25], and material properties of ferrofluids [13,14,18–20,23,24,30–36]. We understand this could make our work of broader interest and eventually help experimentalists to test the predictions of our theoretical model.

The real world parameters that reflect our theoretical regime are now presented. For the typical parameters related to probe-tack experiments we take [4,5]: $k=3.0\times10^5$ N/m, $R_0=5.0\times10^{-2}$ m, $b_0=O(10^{-4})-O(10^{-3})$ m, and $V=7.3\times10^{-7}$ m/s. For the radial magnetic-field configuration [25] we use $a=5.0\times10^{-3}$ m and $H_0=1.6\times10^3$ A/m. We note that the strength of the radial magnetic field generated in Ref. [25] is 1 order of magnitude larger than the one we use. It is also worth pointing out that the plate dimensions of real probe-tack instruments and the size of the radial magnetic-field source are compatible. Although the practical implementation of this composed system (lifting apparatus coupled to a magnetic-field source) might not be straightforward, it is in principle viable.

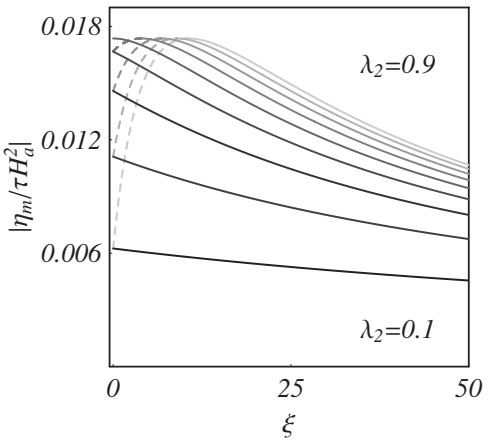

FIG. 2. Magnitude of the normalized magnetoviscous contribution to the shear viscosity as a function of the dimensionless shear ξ. Here $0.1\leq\lambda_2\leq0.9$ in steps of 0.1. Lighter color means higher values of λ_2. The dashed (solid) curves identify a shear thickening (thinning) regime.

Since the magnetic susceptibility of ferrofluids varies in a wide range, namely, from 1 to 80 [13,14,33–35], we take $\chi=5$ as a representative value. Moreover, we consider that 0.1 s$\lesssim\tau\lesssim$1 s [24,36]. In general, the viscosity of a ferrofluid can be tunable for almost any volume fraction of magnetic particles by properly choosing the viscosity of the carrier liquid. The higher the concentration of magnetic particles the more viscous the ferrofluid becomes. Therefore, current ferrofluids have viscosity ranging from 10^{-3} Pa s to 10^2 Pa s [13,14,30–32]. Here we choose a high viscosity ferrofluid with $\eta_0=10^2$ Pa s. By utilizing this set of physical parameters we obtain the following characteristic dimensionless quantities: $N_B=5.0\times10^{-5}$, $N_N=2.5\times10^3$, and $\gamma=10^2$. Note that under such circumstances $N_N\gg N_B$, meaning that the non-Newtonian contribution is of major impact to our problem. The range of values we take for the dimensionless shear parameter ($0\leq\xi\leq50$) is also in line those employed in Refs. [18–20,23,24]. Unless otherwise stated these dimensionless parameters will be used throughout this work.

A. Changes in the viscosity

In this section we look into the details of how the magnetic effects alter the adhesion force. In order to better understand the behavior of the adhesion force, first we examine how the viscosity of the ferrofluid is affected by shear and chain formation. Figure 2 illustrates how the magnitude of the magnetoviscous contribution to the shear viscosity Eq. (9) (in units of τH_a^2) varies as a function of the dimensionless shear ξ, with the chain formation parameter changing from $\lambda_2=0.1$ to $\lambda_2=0.9$ in steps of 0.1. Lighter color indicates higher values of λ_2. First, we recall that since η_m is negative within the interval $0<\lambda_2<1$, the normalized magnetovis-

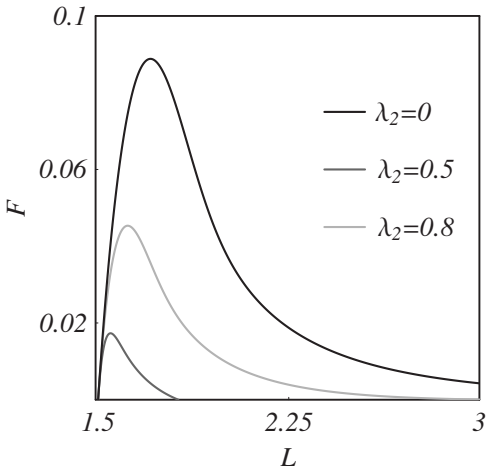

FIG. 3. Adhesion force F for the compliant situation and zero shear, as a function of displacement L, for the initial plate spacing $b_0=1.5$. The color labeling refers to distinct values of λ_2: 0 (black curve), 0.5 (dark gray curve), and 0.8 (light gray curve).

cosity tends to decrease the value of the total viscosity η. Notice that if $\lambda_2<0.5$ the magnitude of the magnetoviscosity is an increasing function of λ_2. Physically, this can be explained on the basis of the alignment of the emerging chains along the local magnetic field, favoring flow in the radial direction. It is also evident that if $\lambda_2<0.5$ the normalized magnetoviscosity decreases with increasing shear, clearly indicating a shear-thinning behavior.

It is worth pointing out that, regardless the value of λ_2, all the curves tend monotonically to zero with increasing shear. This effect is somewhat expected since strong shear destroys the chains, eliminating any non-Newtonian contribution. Roughly speaking, this can be explained by the rupture of the chains (which have been formed due to interparticle interaction) due to strong viscous forces in the shear flow [19].

On the other hand, if $\lambda_2\geq 0.5$ the curves reach their maximum values at nonzero values of shear ($\xi=\xi_{\max}$). Note that all maxima correspond to the same value of the normalized magnetoviscosity. The existence of these maxima leads to a shear-thickening behavior for $\xi<\xi_{\max}$ (dashed curves) and to a shear-thinning situation for $\xi>\xi_{\max}$ (solid curves). Observe that the shear-thickening effect is more significant for larger λ_2 which implies in longer chains. These longer structures are more susceptible to the torque exerted by the elongational flow, suppressing further stretching of the fluid, and consequently leading to higher total viscosity (this happens even at the zero shear situation). In this region ($\xi<\xi_{\max}$) the competition between torque and alignment of the chains results in shear thickening. However, if shear is further increased ($\xi>\xi_{\max}$), the chains tend to be destroyed, weakening the overall non-Newtonian effects, and promoting a shear-thinning regime.

B. Adhesion force: Zero shear limit

We proceed by examining Fig. 3 that presents the force-distance curves for thin layers of a non-Newtonian ferrofluid at the zero shear limit ($\xi\to 0$). By taking this limit we focus on the exclusive influence of magnetic particle chain formation on the adhesive force. Typical force-distance curves increase sharply at initial stages of the plate separation process [3–12]. For an ideal viscous Newtonian liquid, there is no apparent physical reason for the actual force to start at zero, increase quickly to a peak, and then decrease abruptly. However, this behavior can be described as a result of the elasticity of the probe-tack apparatus [3,4]. We address this issue and calculate the complete form of the force-distance curves, considering the intrinsic rigidity of the lifting machine (compliant apparatus situation). To do it, we follow Refs. [3,4,10] and assume that, during the entire separation process, there is a perfect balance between viscous plus ferrohydrodynamic forces and the spring restoring (dimensionless) force $L-b$ which results from the deflection of the apparatus. Using Eq. (14) and the relation $L=b_0+t$ we can write $\dot{b}=db/dL$ so that

$$F(b,\dot{b})=L-b. \tag{15}$$

This nonlinear differential equation is solved numerically for $b(L)$ and we find the force curves from $F=L-b(L)$.

Figure 3 compares the force-distance curve for the case without chain formation ($\lambda_2=0$, black curve), and those in which chains are formed ($\lambda_2=0.5$ and $\lambda_2=0.8$, darker and lighter gray curves, respectively). This is shown for a characteristic initial plate spacing $b_0=1.5$. The most interesting feature of Fig. 3 is actually the role of chain formation in determining the adhesion behavior as λ_2 is changed. As λ_2 varies from zero (black curve) to 0.5 (dark gray curve), the adhesion force is significantly reduced just by the action of chain formation. In fact, there is a 80% shift between the maxima of the force-displacement curves for $\lambda_2=0$ and $\lambda_2=0.5$. Conversely, if λ_2 keeps increasing ($0.5<\lambda_2<1$) the opposite effect takes place, so that adhesion increases and eventually the force tends to the chainless case described by the black curve. The increase in the adhesion force is illustrated by the lighter gray curve for $\lambda_2=0.8$, which is shifted by 65% with respect to the black curve. Note that hidden in the black curve there are in fact two curves that simply overlap, namely, $\lambda_2=0$ and $\lambda_2=1$. Therefore, the zero shear situation is characterized by an "up and down" motion of the force peaks as λ_2 varies from 0 to 1. These results indicate real, potentially observable differences in behavior due to chain formation, since a shift in data as small as 20% is expected to be resolvable by current experimental techniques [37]. In this sense, our modified probe-tack test could work as a useful tool for detecting the presence of magnetic chain formation in ferrofluids. In addition, it could also help to estimate the approximate length of such structures.

A physical explanation for the phenomena depicted in Fig. 3 can be attributed to the magnetoviscous contribution to the shear viscosity as discussed in Fig. 2. In the zero shear limit the coefficients Γ and Λ appearing in the third term on right-hand side of Eq. (14) are independent of λ_2, so that all the contribution due to the formation of chains comes exclusively from the magnetoviscous effect produced by the term multiplied by N_N in Eq. (14). As mentioned earlier in this work, if $\xi=0$ the magnetoviscous contribution to the shear viscosity Eq. (9) reduces to a parabolic function of λ_2 in such

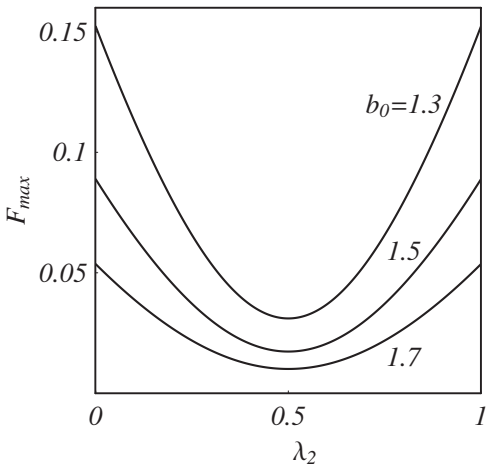

FIG. 4. The maximum value of the adhesion force $F_{\max}$ as a function of λ_2, at the zero shear limit, for three values of b_0: 1.3, 1.5, and 1.7.

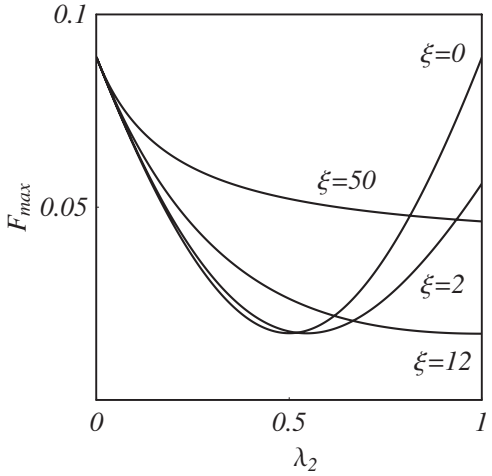

FIG. 5. The maximum value of the adhesion force $F_{\max}$ as a function of λ_2 for $b_0=1.5$, and different values of ξ: 0, 2, 12, and 50.

a way it decreases (increases) if $\lambda_2<0.5$ ($\lambda_2>0.5$). This justifies the behavior shown in Fig. 3 in which the adhesion force decreases for $\lambda_2<0.5$ and increases otherwise. We point out that this sort of argument is also valid for the nonzero shear situation, as we will discuss in Sec. III C. The parabolic behavior mentioned above is even clearer in Fig. 4 that plots the maximum value of the adhesion force ($F_{\max}$) as a function of λ_2 for three different values of b_0. It is also evident that by modifying b_0 no qualitative changes are observed.

C. Adhesion force: Nonzero shear situation

We close our discussion by turning to the nonvanishing shear situation and discuss how it can influence the adhesion force. Rigorously speaking, the dimensionless shear rate is given by $\xi=\dot{b}(L)/b(L)$, being obviously a quantity that varies with L, a fact that introduces some numerical difficulties for the solution of the nonlinear differential Eq. (15). However, through a number of numerical tests we have checked that ξ can be considered as a constant parameter in Eq. (15) if shear is not too large ($\xi\leq 50$). This assumption is consistent with the typical values for the dimensionless shear rate used in previous studies [23,24]. The action of ξ on the force peak ($F_{\max}$) is illustrated in Fig. 5 for $0\leq\lambda_2\leq 1$, and different values of ξ: 0, 2, 12, and 50. For zero shear, as commented earlier, the magnetoviscous contribution for the viscosity varies parabolically with λ_2, making $F_{\max}$ to first decrease ($\lambda_2<0.5$), and then increase ($\lambda_2>0.5$) back to the chainless case value. In general, the behavior of the peaks result from the competition between the magnetoviscous contribution to the adhesion force [second term on the right-hand side of Eq. (14)], and the term proportional to N_B in Eq. (14). It is worth noting that the magnetoviscous term tends to diminish the adhesion force, whereas the other term tends to increase it. Here, since $N_N\gg N_B$ the magnetoviscous contribution takes over.

From Fig. 5 it can also be noticed that for nonzero values of shear the parabolic symmetry with respect to λ_2 is broken. For $\lambda_2<0.5$ the value of $F_{\max}$ always increases with ξ, consistently with the shear-thinning signature of the magnetoviscosity η_m. On the other hand, for a given $\lambda_2\geq 0.5$ and increasingly larger shear, $F_{\max}$ first decreases, reaches a minimum value, and then increases. This behavior takes place due to the transition from a shear-thickening to a shear-thinning regime similarly to what was obtained in Fig. 2. This happens as a result of the prevalence of the magnetoviscous contribution to the adhesion force. If sufficiently higher values of shear are considered, the magnitude of $F_{\max}$ will tend to the chainless case one. This occurs because higher values of shear fragment the chains eliminating all magnetic contributions.

Further illustration about the action of shear on the force-distance curves can be seen in Fig. 6 which depicts F as a function of L for two different values of ξ: (a) 2, and (b) 12, with $b_0=1.5$. These curves should be contrasted with those appearing in Fig. 3 that refers to the zero shear case ($\xi=0$), and the same b_0. If shear is finite and relatively small ($\xi=2$), we notice from Fig. 6(a) that the adhesion force for the lighter gray curve is clearly smaller than the corresponding force strength for the zero shear case illustrated in Fig. 3. Conversely, the dark gray curve is slightly shifted toward larger values. Despite the fact that the minimum value of the force peak is no longer at $\lambda_2=0.5$, the general up and down motion of the peaks is still present. These findings can be checked from the data shown in Fig. 5.

On the other hand, for larger values of shear ($\xi=12$), as shown in Fig. 6(b), the force drop is even more intense for the lighter gray curve, so that now it lies below the dark gray one. Note that the force peak of this curve ($\lambda_2=0.5$) is higher than the equivalent position shown in Fig. 6(a). This last remark is also in agreement with our discussion of Fig. 5. Differently from the $\xi=2$ case the up and down motion of the peaks does not occur, so that by increasing λ_2 the maxima of the adhesion force decrease monotonically. Since in Fig. 6 the relative position of the gray curves are reversed as shear is increased, it is evident that one can observe distinct behaviors for F depending on the shear regime under consideration

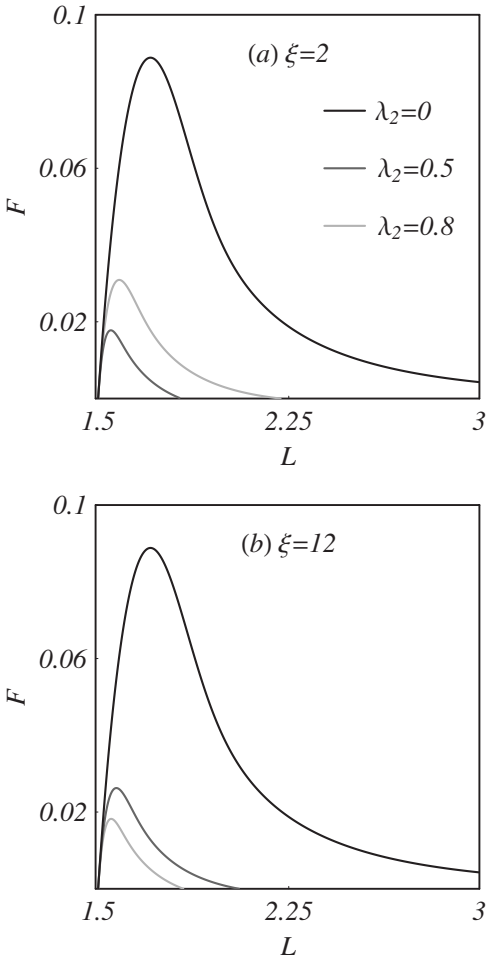

FIG. 6. Adhesion force F for the compliant situation and nonzero shear, as a function of displacement L, for $b_0=1.5$, (a) $\xi=2$, (b) $\xi=12$. The color labeling is the same as the one utilized in Fig. 3.

(low or high). Of course, if shear is increased further the two gray curves tend to overlap and coincide with the black one ($\lambda_2=0$) due to the fragmentation of chains.

IV. CONCLUDING REMARKS

We have investigated the rheological and adhesive responses of a chain-forming ferrofluid under tension submitted to an applied radial magnetic field. For this situation we have examined the interplay of magnetic, shear, and chain formation effects in determining the adhesive strength of the magnetic fluid sample. Our theoretical description is based on a generalized Darcy's law approach in which the fluid's total viscosity includes a magnetoviscous term that conveniently couples shear and magnetic contributions. One peculiar aspect of this magnetoviscosity is its dependence on the length of the magnetic particle chains formed. We have observed that as the length of the chains is allowed to vary, the non-Newtonian ferrofluid can display shear-thinning and shear-thickening behaviors.

The adhesive force is calculated using Darcy's law plus an augmented version of the stress tensor which accounts for the existence of short chains in the ferrofluid. We have studied the adhesive features of the magnetic sample under zero and nonzero shear circumstances. In the zero shear limit, as the length of the chains is increased, we have verified that the adhesion force peak first decreases, reaches a minimum value, and then increases back to the usual chainless situation.

Nevertheless, if shear is nonzero the dependence of the adhesion force on the chain length varies with the magnitude of shear. For small shear values the qualitative behavior of the adhesion force curves is similar to the one observed for the zero shear case. However, for intermediate values of shear the up and down motion of the force peaks does not occur. Instead, the force peaks become lower and lower for increasingly larger values λ_2. Finally, at higher shear values the chains tend to be destroyed, and consequently all adhesion curves approach the chainless situation. All these results indicate that probe-tack tests may become instrumental in checking the existence of chains in ferrofluids, also providing a valid additional method to predict the length of these structures.

Very recently, we have learned that a research group from MIT, led by McKinley [38] has been conducting controllable probe-tack experiments (in plate-plate geometry) using a magnetorheological fluid subjected to an external magnetic field produced by a small cylindrical magnet. Such a complex magnetic fluid [39] exhibits a manifested yield stress character which allows an increased resistance to shear loading regulated by a magnetic field. In addition to its intrinsic scientific and practical importance, this experiment substantiates the plausibility of the magnetically controlled probe-tack setup suggested in this work and also in Ref. [10]. Incidentally, recent stress controlled rheometer experiments [40,41] show the appearance of a magnetic field-dependent yield stress in ferrofluids. Although a theoretical study describing the interplay of yield stress, shear loading, magnetic forces, and magnetic particle chain formation in ferrofluids and magnetorheological fluids is certainly challenging, and still not available, steps toward its theoretical understanding seem as a natural extension of our current work.

In summary, we have shown that the inclusion of the magnetic particle chain formation considerably enriches the rheological properties of the system, leading to the occurrence of interesting adhesive phenomena in magnetic fluids. Our theoretical results point to tangible, potentially observable differences in behavior due to chain formation, adding to the general discussion of the question of magnetic particle chain formation on ferrofluid dynamics.

ACKNOWLEDGMENTS

We thank CNPq (Brazilian Research Council) for financial support of this research through the program "Instituto do Milênio de Fluidos Complexos" under Contract No. 420082/2005-0, and also through the CNPq/FAPESQ Pronex program. We acknowledge useful discussions with R. Ewoldt, G. McKinley, A. Hosoi, A. Lindner, and S. Afkhami.

[1] D. J. Yarusso, in *Adhesion Science and Engineering—The Mechanics of Adhesion*, edited by D. A. Dillard and A. V. Pocius (Elsevier, Amsterdam, 2002).
[2] D. W. Aubrey, in *Aspects of Adhesion*, edited by K. W. Allen (Elsevier, New York, 1988).
[3] B. A. Francis and R. G. Horn, J. Appl. Phys. **89**, 4167 (2001).
[4] D. Derks, A. Lindner, C. Creton, and D. Bonn, J. Appl. Phys. **93**, 1557 (2003).
[5] S. Poivet, F. Nallet, C. Gay, and P. Fabre, Europhys. Lett. **62**, 244 (2003).
[6] S. Poivet, F. Nallet, C. Gay, J. Teisseire, and P. Fabre, Eur. Phys. J. E **15**, 97 (2004).
[7] A. Lindner, D. Derks, and M. J. Shelley, Phys. Fluids **17**, 072107 (2005).
[8] J. A. Miranda, Phys. Rev. E **69**, 016311 (2004).
[9] J. Nase, A. Lindner, and C. Creton, Phys. Rev. Lett. **101**, 074503 (2008).
[10] J. A. Miranda, R. M. Oliveira, and D. P. Jackson, Phys. Rev. E **70**, 036311 (2004).
[11] A. Zosel, Colloid Polym. Sci. **263**, 541 (1985).
[12] H. Lakrout, P. Sergot, and C. Creton, J. Adhes. **69**, 307 (1999).
[13] R. E. Rosensweig, *Ferrohydrodynamics* (Cambridge University Press, Cambridge, 1985).
[14] E. Blums, A. Cebers, and M. M. Maiorov, *Magnetic Fluids* (de Gruyter, New York, 1997).
[15] M. I. Shliomis, Sov. Phys. Usp. **17**, 153 (1974).
[16] M. I. Shliomis, in *Ferrofluids*, Lecture Notes in Physics Vol. 594, edited by S. Odenbach (Springer, Berlin, 2002).
[17] H. W. Müller and M. Liu, Phys. Rev. E **64**, 061405 (2001).
[18] S. Odenbach, J. Phys.: Condens. Matter **16**, R1135 (2004); L. M. Pop and S. Odendach, *ibid.* **18**, S2785 (2006).
[19] S. Odenbach, L. M. Pop, and A. Y. Zubarev, GAMM-Mitteilungen **30**, 195 (2007).
[20] S. Odenbach and H. W. Müller, Phys. Rev. Lett. **89**, 037202 (2002).
[21] A. Y. Zubarev and L. Y. Iskakova, Phys. Rev. E **61**, 5415 (2000); **65**, 061406 (2002).
[22] P. Ilg, E. Coquelle, and S. Hess, J. Phys.: Condens. Matter **18**, S2757 (2006).
[23] O. Müller, D. Hahn, and M. Liu, J. Phys.: Condens. Matter **18**, S2623 (2006).
[24] S. Mahle, P. Ilg, and M. Liu, Phys. Rev. E **77**, 016305 (2008).
[25] W. H. Heiser and J. A. Shercliff, J. Fluid Mech. **22**, 701 (1965).
[26] S. Y. Molokov and J. E. Allen, J. Phys. D: Appl. Phys. **25**, 393 (1992); **25**, 933 (1992).
[27] D. P. Jackson, R. E. Goldstein, and A. O. Cebers, Phys. Rev. E **50**, 298 (1994).
[28] R. B. Bird, R. Armstrong, and O. Hassager, *Dynamics of Polymeric Liquids* (Wiley, New York, 1977).
[29] S. Odenbach and H. W. Müller, J. Magn. Magn. Mater. **289**, 242 (2005).
[30] O. T. Mefford, R. C. Woodward, J. D. Goff, T. P. Vadala, T. G. St. Pierre, J. P. Dailey, and J. S. Riffle, J. Magn. Magn. Mater. **311**, 347 (2007).
[31] S. Afkhami, Y. Renardy, M. Renardy, J. S. Riffle, and T. St Pierre, J. Fluid Mech. **610**, 363 (2008).
[32] See also Ferrotec's homepage http://www.ferrotec.com
[33] J.-C. Bacri, A. Cebers, and R. Perzynski, Phys. Rev. Lett. **72**, 2705 (1994).
[34] D. Rannacher and A. Engel, Phys. Rev. E **69**, 066306 (2004).
[35] R. Perzynski and J.-C. Bacri (private communication).
[36] J. P. Embs, S. May, C. Wagner, A. V. Kityk, A. Leschhorn, and M. Lücke, Phys. Rev. E **73**, 036302 (2006).
[37] R. Ewoldt, G. McKinley, and A. Hosoi (private communication).
[38] R. Ewoldt, G. McKinley, and A. Hosoi, Bull. Am. Phys. Soc. **53** (15), 252 (2008).
[39] See for instance, A. Kawai *et al.* in Proceedings of the Eighth International Conference on Electro-Rheological and Magneto-Rheological Suspensions, edited by G. Bossis (World Scientific, Singapore, 2002).
[40] H. Shahnazian and S. Odenbach, J. Phys.: Condens. Matter **20**, 204137 (2008).
[41] H. Shahnazian and S. Odenbach, Int. J. Mod. Phys. B **21**, 4806 (2007).